ACS Photonics

Letter

pubs.acs.org/journal/apchd5

Second-Harmonic Generation from a Magnetic Buried Interface Enhanced by an Interplay of Surface Plasma Resonances

Ilya Razdolski,*[,†] Sergii Parchenko,[‡] Andrzej Stupakiewicz,[‡] Sergey Semin,[†] Alexander Stognij,[§] Andrzej Maziewski,[‡] Andrei Kirilyuk,[†] and Theo Rasing[†]

[†]Institute for Molecules and Materials, Radboud University Nijmegen, Heyendaalseweg 135, Nijmegen, The Netherlands

[‡]Laboratory of Magnetism, Faculty of Physics, University of Bialystok, Lipowa 41, Bialystok, Poland

[§]Scientific-Practical Materials Research Centre of the NASB, P. Brovki 19, Minsk, Belarus

ABSTRACT: Magnetization-induced second-harmonic generation (SHG) enhanced by surface plasma resonances (SPRs) is studied in a Au/(Bi,Tm) iron garnet (IG) perforated magnetoplasmonic crystal capable of sustaining SPRs at both air/Au and Au/(Bi,Tm)IG interfaces. Asymmetry of a crossing point of the SPR branches is shown, demonstrating a significant difference in the SHG spectra at both sides of the complex resonance. Despite the thick (120 nm) Au layer, the sensitivity of the SHG to the SPR at the buried Au/garnet interface is demonstrated through observing an SHG magnetic contrast, when the SHG is amplified by an excitation of the SPR at the bottom interface.

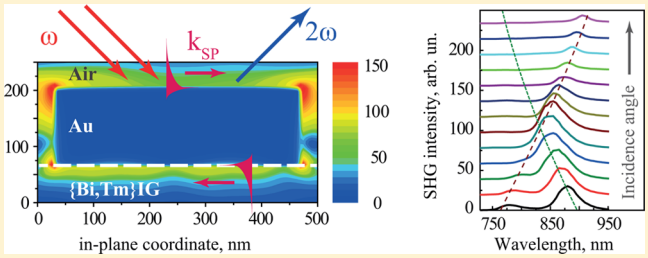

KEYWORDS: *magnetoplasmonics, nonlinear optics, magneto-optics, bismuth-doped iron garnet*

The recent development of magnetoplasmonics has opened up new paths for future research in modern photonics and nanooptics. Significant progress has been made with a straightforward approach, utilizing ferromagnetic transition metals instead of traditional plasmonic materials, such as Au or Ag.[1] In general, two main achievements can be outlined here. First, a sizable enhancement of magneto-optical effects facilitated by the excitation of surface plasmon resonances (SPR) has been widely demonstrated.[2−16] On the other hand, the possibility to control resonant conditions by means of an external magnetic field, originally proposed for magnetoplasmonic materials,[17,18] has shown promising results for possible applications.[19−21] Along with linear optical effects, excitation of the SPRs was found to enhance the magneto-optical effects in second-harmonic generation (SHG)[22−24] and activate new sources of SHG in magnetoplasmonic structures.[25]

Although ferromagnetic transition metals such as Fe, Co, or Ni are the simplest way to merge magneto-optics with plasmonics, electron−electron scattering responsible for the ferromagnetic aligning of spins in such metals leads to a faster decay rate and lower quality factor of any collective electronic excitation such as an SPR. Instead, a sensible approach using a heterostructure of a noble metal with a high-quality SPR and a ferromagnetic dielectric has been proven to yield more promising results for linear[26−35] and nonlinear[36−39] magneto-optics. The periodic perforation in a metal allows for the excitation of a double SPR on the metallic film, when the electric field at both metal−dielectric interfaces is simultaneously enhanced.[40−42] In the case of such a complex excitation, a highly intuitive model has been proposed,[34] suggesting that for a thin metallic film SPRs at both interfaces can be considered as two coupled oscillators. However, little is known about this SPR excitation in a thick metal layer, where the coupling of the overlap of the electromagnetic fields induced by the SPRs at opposite interfaces vanishes.

In this paper, we examine the SHG from a Au/(Bi,Tm) iron garnet (BTIG) magnetoplasmonic crystal, which can sustain SPRs at both sides of the 120 nm thick Au film. We analyze the SHG near the point where the SPR branches at both interfaces cross each other and demonstrate the asymmetry of the crossing point. Despite the large thickness of the Au film, we show how the SHG is sensitive to the SPR excited at the buried Au/garnet interface. The inequality of the interfaces is also shown by studying the nonlinear magneto-optical response. The results of numerical simultations are shown to be in good agreement with the experiment, validating the SPRs excitation picture used in the analysis of the data.

SAMPLES AND EXPERIMENTAL TECHNIQUE

A 100 × 100 μm array of thick (120 nm) Au stripes was deposited on 4 μm BTIG, which was grown on a gallium gadolinium garnet (GGG) [100] substrate. This combination of a noble metal (Au) and a ferromagnetic dielectric (BTIG) was chosen to distinguish between the SPRs excited at both interfaces of the Au film. In the nonlinear optical experiments, the fundamental radiation of a Mai-Tai laser system, tunable in the spectral range of 710−990 nm, excited the sample at oblique incidence from the Au side. The structural parameters

Received: October 15, 2014
Published: January 6, 2015

DOI: 10.1021/ph500382u
ACS Photonics 2015, 2, 20−26

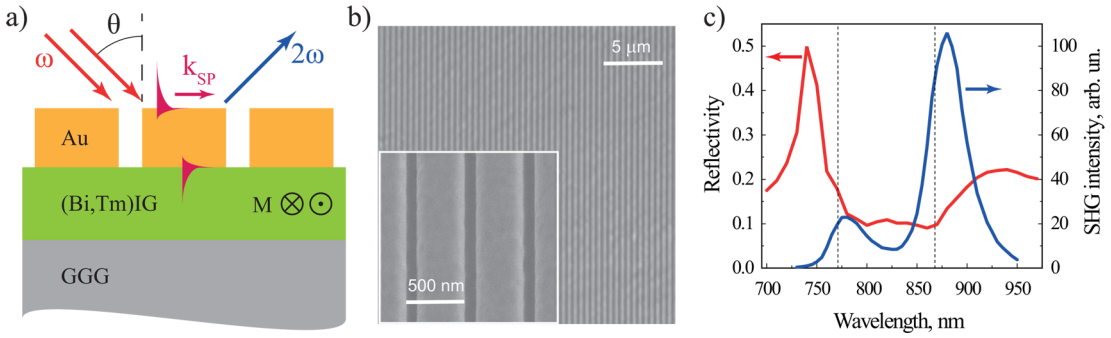

Figure 1. (a) Layout of the sample and experimental schematic. Fundamental p-polarized radiation (red arrows) generates light at double frequency (blue arrow). This process is enhanced by means of the SPR excitation. Magnetic field is applied normal to the plane of the figure. (b) Scanning electron microscope image of the sample. (c) Linear reflectivity (red) and SHG intensity (blue) spectra for 31° of incidence. Vertical dashed lines indicate the spectral positions of the SPRs at the two interfaces of the Au film obtained from eq 1

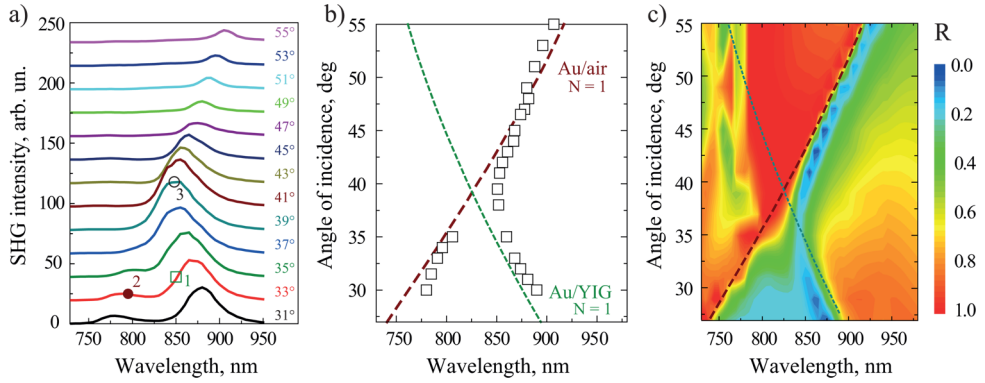

Figure 2. (a) Spectra of SHG intensity registered for a set of angles of incidence. An offset has been added to the curves for clarity. Points 1−3 correspond to the SPR excitation at the bottom (1, Au/BTIG) and top (2, Au/air) interfaces, and the point where both SPRs are excited (3), and are used in further analysis. (b) Resonant angles obtained from the SHG experiments. Dashed green and dark red lines show resonant wavelengths obtained from (1) for the Au/air and Au/BTIG interface, respectively. (c) False color reflectivity (R) plot calculated by means of a finite-difference time domain method. Dashed lines are the same as in (b).

of the sample were chosen so that the crossing point of the two resonance branches was within the tunability range of the laser. The width of the Au stripes was 400 nm, the spatial period was equal to 500 nm, and the Au stripes were perpendicular to the plane of incidence of the incoming radiation (see Figure 1a). The incident radiation was p-polarized, unless stated otherwise, and the registered reflected SHG was always p-polarized. The laser beam at an average power of around 40 mW (repetition rate 82 MHz, pulse duration 100 fs) was tightly focused into a spot of about 10 μm in diameter. The SHG signals were normalized over the square of the incident laser power. The surface morphology and optical image of the Au stripes on the BTIG film were measured by both scanning electron microscopy and optical wide-field polarizing microscopy (see Figure 1b)

EXPERIMENTAL RESULTS

Typical spectral dependences of the linear reflectivity (red) and SHG intensity (blue) are shown in Figure 1c for an angle of incidence of 31°. The two features in the reflectivity correspond to the excitations of the SPRs. At the same time, the SHG spectrum measured in the same experimental conditions shows two distinct peaks around the resonant wavelengths. It is worth noticing that the peak at the higher wavelength, which is the strongest, corresponds to the SPR excitation at the buried Au/BTIG interface. The dashed lines indicate the resonant wavelengths obtained from the well-known relation[43]

$$k_{SP} = k_0 \sin\theta + N\frac{2\pi}{d} \quad (1)$$

where k_{SP} is the k-vector of a surface plasmon, k_0 is the k-vector of light, θ is the angle of incidence, N is an integer, and d is the period of the metallic structure. The k-vector of a plasmon can be calculated if the dielectric functions of both metallic Au (ε_1) and dielectric BTIG (ε_2) layers are known:[44,45]

$$k_{SP} = k_0\sqrt{\frac{\varepsilon_1\varepsilon_2}{\varepsilon_1 + \varepsilon_2}} \quad (2)$$

It is seen in Figure 1 that the agreement between the calculated and observed resonant wavelengths is quite good, given the known mismatch between resonances in the linear and nonlinear optical responses. This mismatch is associated with the symmetric/antisymmetric bound and leaky modes of an SPR, which are in general nondegenerate if the metallic film interfaces feel each other or due to the losses. Only leaky modes can contribute to the SHG output.[46] In order to learn more about the spectral behavior of the SHG signal, we performed systematic measurements at a set of angles of incidence θ from 31° to 55°, which are shown in Figure 2a. Two features can be seen in this figure: first, the typical avoided crossing behavior of the SPR branches, and second, the asymmetry in the SHG enhancement below and above the crossing point. The avoided crossing is even better seen in Figure 2b, where the resonant angles obtained from the SHG

DOI: 10.1021/ph500382u
ACS Photonics 2015, 2, 20−26

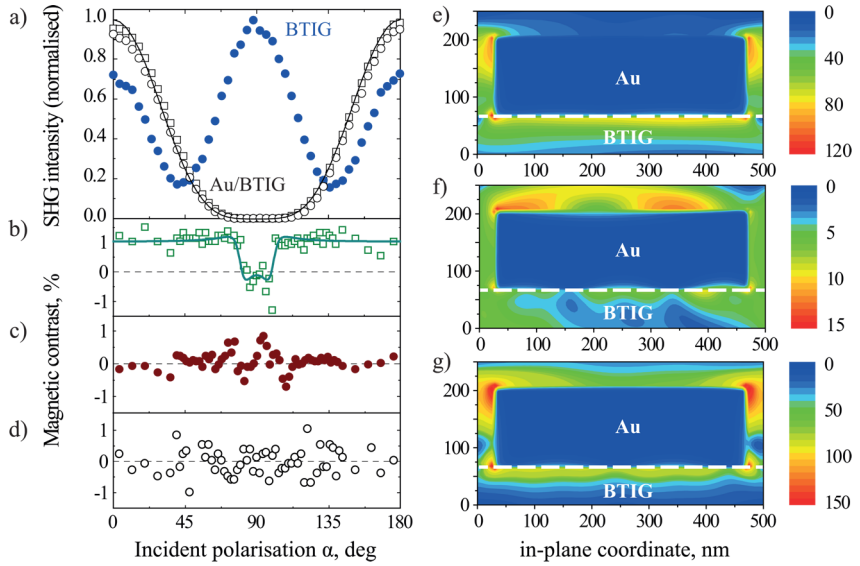

Figure 3. (a) SHG intensity as a function of incident polarization for the points 1 and 2 (see Figure 2) corresponding to the SPR excitation at the two interfaces at 33° of incidence (empty dark squares, 795 nm, and circles, 850 nm) and for the bare BTIG film (solid blue circles). Dark solid line is the fit to the experimental data. (b−d) SHG magnetic contrast ρ as a function of incident polarization for points 1−3 (see Figure 2), corresponding to the excitation of the SPRs at the Au/BTIG buried interface (green squares, 850 nm, 33° of incidence), the Au/air interface (dark red circles, 795 nm, 33° of incidence), and the crossing point of the resonances (open circles, c, 848 nm, 39° of incidence). The solid line in (b) is the fit to the experimental data; see eq 4. (e−g) Optical intensity distributions $|E(x, z)|^2$ in the plane of incidence for points 1−3 (see Figure 2), corresponding to the SPR excitation at the top (e, Au/BTIG) and bottom (f, Au/air), and the point where both SPRs are excited (g). The wavelengths and angles are the same as in (b)−(d). The dielectric permittivities used for the simulations are the following: for Au, $\varepsilon = -28.27 + i1.75$, $-23.66 + i1.48$, $-28.10 + i1.74$ for points 1−3, respectively, while for BTIG a single $\varepsilon = 4.33$ was used.

spectra are plotted with empty squares. Dashed lines correspond to the calculations according to eq 1, indicating the crossing at about 40°. For θ well below that value, two distinct peaks are seen in the SHG spectra. For larger angles, after the avoided crossing only the SPR resonance corresponding to the Au/air interface survives, while the other one vanishes completely. The SHG efficiency plot is found to correlate very well with the results of finite-difference time domain simulations of the linear reflectivity (performed using the Lumerical software) shown in Figure 2c. Two dips at low angles turn into one single dip at incidence angles above the crossing point of the two branches of SPRs.

DISCUSSION

In this section we shall discuss the main question that can be raised regarding the experimental data presented above, which is why and to what extent is the nonlinear optical response of the magnetoplasmonic crystal sensitive to the buried Au/BTIG interface. In order to do this, we shall first address the problem of the interaction of the SPRs excited at the opposite interfaces. Note that in principle a crossing of two such resonance branches can be described within the model of coupled oscillators proposed by Pohl et al.[34] However, the coupling coefficients η_i are strongly dependent on the distance between the interfaces. For an SPR, the penetration depth of the electric field at wavelength λ is given by[43]

$$z_1 = \frac{\lambda}{2\pi}\left(\frac{\varepsilon_1 + \varepsilon_2}{\varepsilon_1^2}\right)^{1/2} \quad (3)$$

where $\varepsilon_{1,2}$ are the real parts of the dielectric permittivity of a metal and dielectric medium, respectively. For Au and 850 nm radiation, it gives 25 and 23 nm for the Au/air and Au/BTIG interfaces, respectively. As such, it is hard to expect that the 120 nm thick Au stripe can sustain mutually correlated oscillations at both interfaces with a reasonable coupling strength. This consideration leads us again to the question of the origin of the SHG signals, which shall be discussed below.

Obviously, the nonlinear optical response of a magnetoplasmonic crystal is determined by its geometrical parameters. Similar SHG spectra have been observed for the sample with a Au film pitch of 600 nm instead of 500 nm. The only essential difference is, of course, the spectral position of the resonances. Much richer options can be obtained by varying the thickness of the Au film, thus playing with the interaction of the SPRs excited at opposite interfaces. It is known though that at low thicknesses waveguide modes start to manifest themselves in the spectra.[35] On the other hand, it is clear that, once the Au film is thick enough, the sensitivity to the bottom interface will have been lost. Apparently, the SPR field penetration depths given by eq 3 are not a good reference to the critical thickness, and there is no experimental data on samples with a thicker metallic layer.

It is known that buried interfaces can contribute to linear optical spectra.[47,48] The effect of extraordinary transmission and related Wood anomalies[49] has been studied quite extensively from both experimental[50−54] and theoretical[55−63] points of view. The incident radiation couples to an SPR at the interface on the other side of the metallic film, depleting the incident beam, which leads to the observed features in the reflectivity spectrum, facilitated by the interference of light. However, this idea, though working very well in the case of linear optics, fails to describe the enhancement of SHG when these resonances are excited. Indeed, once the fundamental radiation is resonantly coupled to the bottom interface, local field enhancement $L(\omega)$ leads to an efficient nonlinear optical frequency conversion.[64] However, when the polarization at the double frequency is excited in such a way, the SH radiation

DOI: 10.1021/ph500382u
ACS Photonics 2015, 2, 20−26

generated at the bottom interface cannot exit back through the Au film because the resonant conditions at 2ω are very different. Numerical simulations show that the off-resonant transmission of the SH radiation through the Au film in the discussed spectral range stays at the level of 5−7%, which cannot explain the strong SHG enhancement at the resonance for the fundamental radiation.

Therefore, the question of the enhancement of the reflected SHG when an SPR at the Au/BTIG interface is excited requires further investigation. Probing with s-polarized fundamental light excites no SPR, which is seen as an absence of any resonant features in the spectra and much lower intensity of the SHG signals (not shown). However, a garnet film also has a sizable nonlinear optical susceptibility, which can give rise to the total SHG signal. In order to verify this, we performed a series of measurements of the SHG output as a function of incident polarization α, which was rotated by means of a half-wavelength plate. The result for both resonances excited at $\theta = 33°$ is shown in Figure 3a with empty squares (λ = 795 nm) and circles (λ = 850 nm). The dark solid line represents the $\cos^4 \alpha$ fit, assuming that the p-polarized fundamental beam yields the dominant contribution to the p-polarized SHG signal.[65] At the same time, solid blue circles show the polarization dependence of the p-polarized SHG from the bare garnet. The totally different shape of the dependences indicates that even when the SPR at the bottom interface is excited, the nonlinear optical signal comes from Au only. This is in line with previous findings, where an SPR excitation induces large electric field gradients, thus facilitating the nonlocal SHG from the metallic layer.[22,23,25]

Despite the fact that the main contribution of the SHG comes from the metallic layer, a key to distinguish the SPRs excited at opposite interfaces is the magnetization-induced SHG. In a medium with nonzero magnetization M, the total light intensity at frequency 2ω is given by $I^{2\omega} = |E^{2\omega}_{\text{even}} \pm E^{2\omega}_{\text{odd}}(\pm M)|^2$. In the transverse Kerr geometry (magnetic field is applied in the plane of the sample and perpendicular to the plane of incidence), an interference of the even and odd (in magnetization) terms results in the magneto-optical SHG contrast ρ. The latter, often used as a figure of merit for the magnetization-induced SHG, is given by

$$\rho = \frac{I^{\uparrow} - I^{\downarrow}}{I^{\uparrow} + I^{\downarrow}} \tag{4}$$

where $I^{\uparrow}$ and $I^{\downarrow}$ are the SHG intensities for the two opposite directions of the magnetization. It is known that in the case of SPR excitation the transverse magnetization can affect the SHG twofold: (1) odd and even in magnetization $\chi^{(2)}$ components are enhanced with an inequal efficiency, which modifies the SHG magnetic contrast,[66] and (2) the phase between even and odd in magnetization components can be strongly modified.[25,67] Both of these mechanisms can alter the magneto-optical SHG response at the SPR wavelength significantly. At the same time, it is also known that the transversal magnetization additively contributes to the k-vector of a plasmon, which results in a magnetization-induced shift of the SPR resonant conditions.[55,68] However, in our experiments SHG spectra obtained for the two opposite directions of magnetizations demonstrated no noticeable offset, indicating that the effect in Au/BTIG is apparently too small to be detected. Of course, the considerations regarding the interaction of SPRs at both interfaces are valid in a nonmagnetic case as well.

In nonresonant conditions, no magneto-optical effects in SHG were registered in our experiments. This indicates that if no SPR is excited, the total nonlinear optical signal comes from the top Au/air interface. The data shown in Figure 3b−d demonstrate how the contrast ρ depends on the incident polarization or, which is the same, the efficiency of the SPR excitation. It is seen that when the SPR at the bottom (Au/BTIG) interface is excited, there is a magneto-optical contrast ρ of about 1% if the SHG radiation is p-polarized (Figure 3b). However, an excitation of the SPR at the nonmagnetic Au/air interface yields no magnetic SHG contrast for any polarization of the fundamental light (Figure 3c). The same is observed at the point where the SPR branches cross each other (Figure 3d).

The data shown in Figure 3b demonstrate a relatively low experimental noise, as compared to Figure 3c,d, because the former has been measured with longer time averaging. This has been done in order to fit the magnetic contrast polarization dependence (shown with the solid line) and get better fit parameters. For an abritrary polarization angle α, we can write the total SHG field $E^{2\omega}_t$ as a sum of the electric fields generated by p- and s-polarized fundamental beams $E_{p,s}$, assuming the absence of cross-terms: $E^{2\omega\uparrow,\downarrow}_t = E^{\uparrow,\downarrow}_t \cos^2 \alpha + E^{\uparrow,\downarrow}_t \sin^2 \alpha$. Thus, the total SHG intensity is given by $I_t = |E^{2\omega}_t|^2 = I_p \cos^4 \alpha + I_s \sin^4 \alpha + 2(I_p I_s)^{1/2} \cos^2 \alpha \sin^2 \alpha \cos \varphi$, where $I_{p,s}$ are the SHG intensities for pure p- and s-polarized fundamental beams, respectively, and φ is the phase shift between E_p and E_s. From this, a bulky expression for the magnetic contrast can be obtained with the help of eq 4. For the special case of $\rho_p \ll 1$, $\rho_s \ll 1$, we can use $I^{\uparrow}_i + I^{\downarrow}_i \approx 2I_i$, i = p,s and $((1 - \rho)/(1 + \rho))^{1/2} \approx 1 - \rho$ and thus get

$$\rho(\alpha) \approx \frac{\rho_p + \rho_s \xi \tan^4 \alpha + \sqrt{\xi}(\rho_p + \rho_s)\tan^2 \alpha \cos \varphi}{1 + \xi \tan^4 \alpha + 2\sqrt{\xi}\tan^2 \alpha \cos \varphi} \tag{5}$$

Here the only parameters left are the magnetic contrasts of the SHG generated by p- and s-polarized fundamental beams ρ_p and ρ_s, the phase shift φ, and the ratio $\xi = I_s/I_p$, which can be measured independently. The fitting procedure yields $\xi = 2 \times 10^{-3}$, in agreement with the experimental value of 1.7×10^{-3}. The good quality of the fit was obtained for a p-contrast of $\rho_p \approx 0.01$, while the nonzero value of $\rho_s \approx -0.002$ probably lies within the experimental error bar. It is seen that when the SPR at the buried Au/BTIG interface is excited (otherwise magnetization-insensitive), SHG acquires a noticeable contribution that is dependent on the magnetization of BTIG. No magnetic contrast was observed for the case of a continuous Au film of the same thickness on BTIG. Because no SPR can be excited on such a film in similar experimental conditions, this means that no SHG contribution from the bottom interface, which would be magnetic, can be detected in the experiments. As such, the magnetization-dependent nature of the SHG from the buried Au/BTIG interface is visualized only by means of the SPR excitation.

The relatively low value of the magnetic contrast, ρ = 0.01 (for the bare BTIG ρ was found to reach 0.15), cannot be fully explained by a large nonmagnetic background SHG contribution coming from the top Au interface. First, the spectra shown in Figure 2a demonstrate that the SHG signal is more efficiently enhanced due to the SPR at the bottom Au/BTIG interface than to the one at the top air/Au interface. However, when an SPR is excited at the bottom interface, the SHG sources at the

DOI: 10.1021/ph500382u
ACS Photonics 2015, 2, 20−26

top interface still contribute to the total SHG intensity. As such, the total SHG output can be determined by an interference of two or more terms, and comparison between the absolute values of the SHG signal can be misleading. In order to avoid this confusion, we note that the SPR-induced enhancement of the SHG signals can be primarily attributed to the enhancement of the local field $L(\omega)$, which can be obtained from numerical simulations. Figure 3e−g show the calculated spatial intensity distributions $|E|^2$ for the points 1−3 discussed above, corresponding to the SPR excitation at the bottom (e, Au/BTIG, 850 nm, 33° of incidence) and top (f, Au/air,795 nm, 33° of incidence) interfaces, as well as the double SPR excitation (g, 848 nm, 39° of incidence).

The area shown here is periodic in its horizontal dimension, so that similar hot spots are seen around every Au bar. Note the difference in the scale to the right of each panel, where the intensity of the incident radiation is set to 1. It is seen that the SPR-induced enhancement of the $|E|^2$ and likewise the SHG output at the top (nonmagnetic) interface is not as efficient as that at the bottom interface. This clearly shows that the strong nonmagnetic SHG contribution from the top (Au/air) interface cannot account for low values of the magnetic contrast ρ. Instead, one should consider other sources of nonmagnetic SHG. Likely, in a fashion similar to ref 25, a highly efficient SPR excitation at the bottom interface inevitably leads to large electric field gradients, thus facilitating a strong nonlocal quadrupole SHG. The latter, coming predominantly from Au, is nonmagnetic, which is responsible for the low values of the SHG magnetic contrast ρ_p detected in the experiments.

We would like to note that because the results presented here are obtained with the help of femtosecond laser pulses, it would be of great interest to probe the ultrafast dynamics of these complex plasmon excitations, along the lines discussed in refs 69 and 70. An optical control of the magnetoplasmonic properties can thus be realized by means of nonlinear optics, giving multiple possibilities of optiplasmonic applications. Moreover, the characteristic time scale of plasmon interaction is not known yet, and these studies could trigger significant progress in ultrafast nonlinear plasmonics.

To summarize, we studied SHG in the vicinity of a crossing point of two SPR branches at both sides of the Au film deposited on BTIG. The asymmetry of the excitation wavelength-angle dependence was demonstrated by means of the SHG spectral measurements and numerical simulations. The sensitivity of the SHG to the SPR at the buried Au/BTIG interface was demonstrated by means of magnetization-induced SHG. The SHG magnetic contrast of about 1% was registered for p-polarized fundamental light, when the SHG is facilitated by the excitation of the SPR at the buried interface. Numerical simulations showed that the SHG enhancement due to the excitation of an SPR at the buried interface is likely to be related to the SPR-induced activation of a nonlocal SHG source.

AUTHOR INFORMATION

Corresponding Author

*E-mail: i.razdolski@science.ru.nl.

Notes

The authors declare no competing financial interest.

ACKNOWLEDGMENTS

This work has been supported by the Seventh Framework Program (EU-FP7) Grant No. NMP-3-LA-2010-246102 (IFOX Project), the European Research Council ERC Grant Agreement No. 339813 (Exchange), and the SYMPHONY project operated within the Foundation for Polish Science Team Programme cofinanced by the EU European Regional Development Fund, OPIE 2007−2013.

REFERENCES

(1) Armelles, G.; Cebollada, A.; García-Martín, A.; González, M. U. Magnetoplasmonics: combining magnetic and plasmonic functionalities. *Adv. Opt. Mater.* **2013**, *1*, 10−35.

(2) Feil, H.; Haas, C. Magneto-optical Kerr effect, enhanced by the plasma resonance of charge carriers. *Phys. Rev. Lett.* **1987**, *58*, 65−68.

(3) Safarov, V.; Kosobukin, V.; Hermann, C.; Lampel, G.; Peretti, J.; Marliere, C. Magneto-optical effects enhanced by surface plasmons in metallic multilayer films. *Phys. Rev. Lett.* **1994**, *73*, 3584−3587.

(4) Fumagalli, P.; Spaeth, C.; Rudiger, U. A new magneto-optic enhancement effect in macroscopic ferrimagnets. *IEEE Trans. Magn.* **1995**, *31*, 3319−3324.

(5) Hermann, C.; Kosobukin, V. A.; Lampel, G.; Peretti, J.; Safarov, V. I.; Bertrand, P. Surface-enhanced magneto-optics in metallic multilayer films. *Phys. Rev. B* **2001**, *64*, 235422.

(6) Wurtz, G. A.; Hendren, W.; Pollard, R.; Atkinson, R.; Le Guyader, L.; Kirilyuk, A.; Rasing, T.; Smolyaninov, I. I.; Zayats, A. V. Controlling optical transmission through magneto-plasmonic crystals with an external magnetic field. *New J. Phys.* **2008**, *10*, 105012.

(7) Ctistis, G.; Papaioannou, E.; Patoka, P.; Gutek, J.; Fumagalli, P.; Giersig, M. Optical and magnetic properties of hexagonal arrays of subwavelength holes in optically thin cobalt films. *Nano Lett.* **2009**, *9*, 1−6.

(8) Clavero, C.; Yang, K.; Skuza, J. R.; Lukaszew, R. A. Magnetic field modulation of intense surface plasmon polaritons. *Opt. Express* **2010**, *18*, 7743−7752.

(9) Grunin, A. A.; Zhdanov, A. G.; Ezhov, A. A.; Ganshina, E. A.; Fedyanin, A. A. Surface-plasmon-induced enhancement of magneto-optical Kerr effect in all-nickel subwavelength nanogratings. *Appl. Phys. Lett.* **2010**, *97*, 261908.

(10) Papaioannou, E. T.; Kapaklis, V.; Patoka, P.; Giersig, M.; Fumagalli, P.; Garcia-Martin, A.; Ferreiro-Vila, E.; Ctistis, G. Magneto-optic enhancement and magnetic properties in Fe antidot films with hexagonal symmetry. *Phys. Rev. B* **2010**, *81*, 054424.

(11) Papaioannou, E. T.; Kapaklis, V.; Melander, E.; Hjorvarsson, B.; Pappas, S. D.; Patoka, P.; Giersig, M.; Fumagalli, P.; Garcia-Martin, A.; Ctistis, G. Surface plasmons and magneto-optic activity in hexagonal Ni anti-dot arrays. *Opt. Express* **2011**, *19*, 23867−23877.

(12) Bonanni, V.; Bonetti, S.; Pakizeh, T.; Pirzadeh, Z.; Chen, J.; Nogués, J.; Vavassori, P.; Hillenbrand, R.; Åkerman, J.; Dmitriev, A. Designer magnetoplasmonics with nickel nanoferromagnets. *Nano Lett.* **2011**, *11*, 5333−5338.

(13) Chetvertukhin, A. V.; Grunin, A. A.; Baryshev, A. V.; Dolgova, T. V.; Uchida, H.; Inoue, M.; Fedyanin, A. A. Magneto-optical Kerr effect enhancement at the Wood's anomaly in magnetoplasmonic crystals. *J. Magn. Magn. Mater.* **2012**, *324*, 3516−3518.

(14) Grunin, A. A.; Sapoletova, N. A.; Napolskii, K. S.; Eliseev, A. A.; Fedyanin, A. A. Magnetoplasmonic nanostructures based on nickel inverse opal slabs. *J. Appl. Phys.* **2012**, *111*, 07A948.

(15) Caballero, B.; García-Martín, A.; Cuevas, J. C. Generalized scattering-matrix approach for magneto-optics in periodically patterned multilayer systems. *Phys. Rev. B* **2012**, *85*, 245103.

(16) Melander, E.; Ostman, E.; Keller, J.; Schmidt, J.; Papaioannou, E. T.; Kapaklis, V.; Arnalds, U. B.; Caballero, B.; Garcia-Martin, A.; Cuevas, J. C.; Hjörvarsson, B. Influence of the magnetic field on the plasmonic properties of transparent Ni anti-dot arrays. *Appl. Phys. Lett.* **2010**, *101*, 063107.

(17) Chiu, K. W.; Quinn, J. J. Magnetoplasma surface waves in metals. *Phys. Rev. B* **1972**, *5*, 4707−4709.

DOI: 10.1021/ph500382u
ACS Photonics 2015, 2, 20−26

(18) Ferguson, P.; Stafsudd, O.; Wallis, R. Enhancement of the transverse Kerr magneto-optic effect by surface magnetoplasma waves. *Phys. B+C (Amsterdam, Neth.)* **1977**, *89*, 91−94.
(19) Temnov, V. V.; Armelles, G.; Woggon, U.; Guzatov, D.; Cebollada, A.; Garcia-Martin, A.; Garcia-Martin, J.-M.; Thomay, T.; Leitenstorfer, A.; Bratschitsch, R. Active magneto-plasmonics in hybrid metal−ferromagnet structures. *Nat. Photonics* **2010**, *4*, 107−111.
(20) Manera, M.; Taurino, A.; Catalano, M.; Rella, R.; Caricato, A.; Buonsanti, R.; Cozzoli, P.; Martino, M. Enhancement of the optically activated $\{NO_2\}$ gas sensing response of brookite TiO_2 nanorods/nanoparticles thin films deposited by matrix-assisted pulsed-laser evaporation. *Sens. Actuators, B* **2012**, *161*, 869−879.
(21) Martín-Becerra, D.; Armelles, G.; González, M. U.; García-Martín, A. Plasmonic and magnetoplasmonic interferometry for sensing. *New J. Phys.* **2013**, *15*, 085021.
(22) Tessier, G.; Malouin, C.; Georges, P.; Brun, A.; Renard, D.; Pavlov, V. V.; Meyer, P.; Ferre, J.; Beauvillain, P. Magnetization-induced second-harmonic generation enhanced by surface plasmons in ultrathin Au═Co═Au metallic films. *Appl. Phys. B: Laser Opt.* **1999**, *68*, 545−548.
(23) Pavlov, V. V.; Tessier, G.; Malouin, C.; Georges, P.; Brun, A.; Renard, D.; Meyer, P.; Ferre, J.; Beauvillain, P. Observation of magneto-optical second-harmonic generation with surface plasmon excitation in ultrathin Au/Co/Au films. *Appl. Phys. Lett.* **1999**, *75*, 190−192.
(24) Murzina, T.; Misuryaev, T.; Kravets, A.; Guedde, J.; Schuhmacher, D.; Marowsky, G.; Nikulin, A.; Aktsipetrov, O. Nonlinear magneto-optical Kerr effect and plasmon-assisted SHG in magnetic nanomaterials exhibiting giant magnetoresistance. *Surf. Sci.* **2001**, *482−485*, 1101−1106.
(25) Razdolski, I.; Gheorghe, D. G.; Melander, E.; Hjörvarsson, B.; Patoka, P.; Kimel, A. V.; Kirilyuk, A.; Papaioannou, E. T.; Rasing, T. Nonlocal nonlinear magneto-optical response of a magnetoplasmonic crystal. *Phys. Rev. B* **2013**, *88*, 075436.
(26) Bremer, J.; Vaicikauskas, V.; Hansteen, F.; Hunderi, O. Influence of surface plasmons on the Faraday effect in bismuth-substituted yttrium iron garnet films. *J. Appl. Phys.* **2001**, *89*, 6177−6182.
(27) Khanikaev, A. B.; Baryshev, A. V.; Fedyanin, A. A.; Granovsky, A. B.; Inoue, M. Anomalous Faraday effect of a system with extraordinary optical transmittance. *Opt. Express* **2007**, *15*, 6612−6622.
(28) Belotelov, V. I.; Doskolovich, L. L.; Zvezdin, A. K. Extraordinary magneto-optical effects and transmission through metal-dielectric plasmonic systems. *Phys. Rev. Lett.* **2007**, *98*, 077401.
(29) Belotelov, V. I.; Akimov, I. A.; Pohl, M.; Kotov, V. A.; Kasture, S.; Vengurlekar, A. S.; Gopal, A. V.; Yakovlev, D. R.; Zvezdin, A. K.; Bayer, M. Enhanced magneto-optical effects in magnetoplasmonic crystals. *Nat. Nanotechnol.* **2011**, *6*, 370−376.
(30) Kreilkamp, L. E.; Belotelov, V. I.; Chin, J. Y.; Neutzner, S.; Dregely, D.; Wehlus, T.; Akimov, I. A.; Bayer, M.; Stritzker, B.; Giessen, H. Waveguide-plasmon polaritons enhance transverse magneto-optical Kerr effect. *Phys. Rev. X* **2013**, *3*, 041019.
(31) Belotelov, V. I.; et al. Plasmon-mediated magneto-optical transparency. *Nat. Commun.* **2013**, *4*, 2128.
(32) Chin, J. Y.; Steinle, T.; Wehlus, T.; Dregely, D.; Weiss, T.; Belotelov, V. I.; Stritzker, B.; Giessen, H. Nonreciprocal plasmonics enables giant enhancement of thin-film Faraday rotation. *Nat. Commun.* **2013**, *4*, 1599.
(33) Belotelov, V. I.; et al. Magnetophotonic intensity effects in hybrid metal-dielectric structures. *Phys. Rev. B* **2014**, *89*, 045118.
(34) Pohl, M.; Kreilkamp, L. E.; Belotelov, V. I.; Akimov, I. A.; Kalish, A.; Khokhlov, N. E.; Yallapragada, V. J.; Gopal, A. V.; Nur-E-Alam, M.; Vasiliev, M.; Yakovlev, D. R.; Alameh, K.; Zvezdin, A.; Bayer, M. Tuning of the transverse magneto-optical Kerr effect in magneto-plasmonic crystals. *New J. Phys.* **2013**, *15*, 075024.
(35) Chekhov, A. L.; Krutyanskiy, V. L.; Shaimanov, A. N.; Stognij, A. I.; Murzina, T. V. Wide tunability of magnetoplasmonic crystals due to excitation of multiple waveguide and plasmon modes. *Opt. Express* **2014**, *22*, 17762−17768.
(36) Airola, M.; Liu, Y.; Blair, S. Second-harmonic generation from an array of sub-wavelength metal apertures. *J. Opt. A: Pure Appl. Opt.* **2005**, *7*, S118.
(37) van Nieuwstadt, J. A. H.; Sandtke, M.; Harmsen, R. H.; Segerink, F. B.; Prangsma, J. C.; Enoch, S.; Kuipers, L. Strong modification of the nonlinear optical response of metallic subwavelength hole arrays. *Phys. Rev. Lett.* **2006**, *97*, 146102.
(38) Lesuffleur, A.; Kumar, L. K. S.; Gordon, R. Enhanced second harmonic generation from nanoscale double-hole arrays in a gold film. *Appl. Phys. Lett.* **2006**, *88*, 261104.
(39) Vincenti, M. A.; de Ceglia, D.; Roppo, V.; Scalora, M. Harmonic generation in metallic, GaAs-filled nanocavities in the enhanced transmission regime at visible and UV wavelengths. *Opt. Express* **2011**, *19*, 2064−2078.
(40) Belotelov, V.; Zvezdin, A. Magnetooptics and extraordinary transmission of the perforated metallic films magnetized in polar geometry. *J. Magn. Magn. Mater.* **2006**, *300*, e260−e263.
(41) McMahon, J. M.; Henzie, J.; Odom, T. W.; Schatz, G. C.; Gray, S. K. Tailoring the sensing capabilities of nanohole arrays in gold films with Rayleigh anomalysurface plasmon polaritons. *Opt. Express* **2007**, *15*, 18119−18129.
(42) Lozovskii, V.; Schrader, S.; Tsykhonya, A. Possibility of surface plasmon-polaritons amplification by direct current in two-interface systems with 2D Bragg structure on the surface. *Opt. Commun.* **2009**, *282*, 3257−3265.
(43) Raether, H. *Surface Plasmons*; Springer-Verlag: Berlin, 1988.
(44) Johnson, P. B.; Christy, R. W. Optical constants of the noble metals. *Phys. Rev. B* **1972**, *6*, 4370−4379.
(45) Wijn, H., Ed. *Landolt-Börnstein, Numerical Data and Functional Relationships in Science and Technology, New Series - Group III Condensed Matter*; Springer-Verlag: Berlin, 1991; Vol. *27e*.
(46) Grosse, N. B.; Heckmann, J.; Woggon, U. Nonlinear plasmon-photon interaction resolved by k-space spectroscopy. *Phys. Rev. Lett.* **2012**, *108*, 136802.
(47) Ebbesen, T. W.; Lezec, H. J.; Ghaemi, H. F.; Thio, T.; Wolff, P. A. Extraordinary optical transmission through sub-wavelength hole arrays. *Nature* **1998**, *391*, 667−669.
(48) Genet, C.; Ebbesen, T. W. Light in tiny holes. *Nature* **2007**, 39−46.
(49) Wood, R. W. Anomalous diffraction gratings. *Phys. Rev.* **1935**, *48*, 928−936.
(50) Ghaemi, H. F.; Thio, T.; Grupp, D. E.; Ebbesen, T. W.; Lezec, H. J. Surface plasmons enhance optical transmission through subwavelength holes. *Phys. Rev. B* **1998**, *58*, 6779−6782.
(51) Barbara, A.; Quémerais, P.; Bustarret, E.; Lopez-Rios, T. Optical transmission through subwavelength metallic gratings. *Phys. Rev. B* **2002**, *66*, 161403.
(52) Matsui, T.; Agrawal, A.; Nahata, A.; Vardeny, Z. V. Transmission resonances through aperiodic arrays of subwavelength apertures. *Nature* **2007**, *446*, 517−521.
(53) Søndergaard, T.; Bozhevolnyi, S. I.; Novikov, S. M.; Beermann, J.; Devaux, E.; Ebbesen, T. W. Extraordinary optical transmission enhanced by nanofocusing. *Nano Lett.* **2010**, *10*, 3123−3128.
(54) Beermann, J.; Søndergaard, T.; Novikov, S. M.; Bozhevolnyi, S. I.; Devaux, E.; Ebbesen, T. W. Field enhancement and extraordinary optical transmission by tapered periodic slits in gold films. *New J. Phys.* **2011**, *13*, 3112−3114.
(55) Strelniker, Y. M.; Bergman, D. J. Optical transmission through metal films with a subwavelength hole array in the presence of a magnetic field. *Phys. Rev. B* **1999**, *59*, R12763−R12766.
(56) Porto, J. A.; García-Vidal, F. J.; Pendry, J. B. Transmission resonances on metallic gratings with very narrow slits. *Phys. Rev. Lett.* **1999**, *83*, 2845−2848.
(57) Martín-Moreno, L.; García-Vidal, F. J.; Lezec, H. J.; Pellerin, K. M.; Thio, T.; Pendry, J. B.; Ebbesen, T. W. Theory of extraordinary optical transmission through subwavelength hole arrays. *Phys. Rev. Lett.* **2001**, *86*, 1114−1117.
(58) Sarrazin, M.; Vigneron, J.-P.; Vigoureux, J.-M. Role of Wood anomalies in optical properties of thin metallic films with a

DOI: 10.1021/ph500382u
ACS Photonics 2015, 2, 20−26

bidimensional array of subwavelength holes. *Phys. Rev. B* **2003**, *67*, 085415.
(59) Pendry, J. B.; Martín-Moreno, L.; Garcia-Vidal, F. J. Mimicking surface plasmons with structured surfaces. *Science* **2004**, *305*, 847−848.
(60) Borisov, A. G.; García de Abajo, F. J.; Shabanov, S. V. Role of electromagnetic trapped modes in extraordinary transmission in nanostructured materials. *Phys. Rev. B* **2005**, *71*, 075408.
(61) Strelniker, Y. M.; Bergman, D. J. Transmittance and transparency of subwavelength-perforated conducting films in the presence of a magnetic field. *Phys. Rev. B* **2008**, *77*, 205113.
(62) Delgado, V.; Marqués, R.; Jelinek, L. Analytical theory of extraordinary optical transmission through realistic metallic screens. *Opt. Express* **2010**, *18*, 6506−6515.
(63) Strelniker, Y. M.; Bergman, D. J. Strong angular magneto-induced anisotropy of Voigt effect in metal-dielectric metamaterials with periodic nanostructures. *Phys. Rev. B* **2014**, *89*, 125312.
(64) Simon, H. J.; Mitchell, D. E.; Watson, J. G. Optical second-harmonic generation with surface plasmons in silver films. *Phys. Rev. Lett.* **1974**, *33*, 1531−1534.
(65) Bennemann, K.-H. *Nonlinear Optics in Metals*; Oxford University Press, 1998.
(66) Krutyanskiy, V.; Kolmychek, I.; Ganshina, E.; Murzina, T.; Evans, P.; Pollard, R.; Stashkevich, A.; Wurtz, G.; Zayats, A. Plasmonic enhancement of nonlinear magneto-optical response in nickel nanorod metamaterials. *Phys. Rev. B* **2013**, *87*, 035116.
(67) Zheng, W.; Hanbicki, A.; Jonker, B. T.; Lüpke, G. Control of magnetic contrast with nonlinear magneto-plasmonics. *Sci. Rep.* **2014**, *4*, 1−5.
(68) Kushwaha, M. S.; Halevi, P. Magnetoplasmons in thin films in the Voigt configuration. *Phys. Rev. B* **1987**, *36*, 5960−5967.
(69) Kauranen, M.; Zayats, A. V. Nonlinear plasmonics. *Nat. Photonics* **2012**, *6*, 737−748.
(70) Temnov, V. V. Ultrafast acousto-magneto-plasmonics. *Nat. Photonics* **2012**, *6*, 728−736.

DOI: 10.1021/ph500382u
ACS Photonics 2015, 2, 20−26